Single- and double-electron-capture collision of C^{q+} ($q=3,4$) with CO at keV energies

Hui Gao and Victor H. S. Kwong

Department of Physics, University of Nevada, Las Vegas, 4505 Maryland Parkway, Las Vegas, Nevada 89154-4002, USA
(Received 21 October 2003; published 20 May 2004)

Absolute total single- and double-electron-capture cross sections for C^{q+} ($q=3,4$) with CO have been measured at ~ 0.5 keV/amu using a reflection-time-of-flight mass spectrometer with a laser ablation ion source. The single- and double-electron-capture cross sections for C^{3+} with CO at 423 ± 48 eV/amu are found to be $(0.96\pm0.12)\times10^{-15}$ cm^2 and $(0.99\pm0.13)\times10^{-15}$ cm^2, respectively. The single- and double-electron-capture cross sections for C^{4+} with CO at 565 ± 65 eV/amu are measured to be $(3.16\pm0.42)\times10^{-15}$ cm^2 and $(1.05\pm0.21)\times10^{-15}$ cm^2, respectively. This suggests that double capture should not be ignored in modeling the emission from cascading processes in comet atmosphere.

I. INTRODUCTION

Electron capture during collisions between multiply charged ions and neutral atoms and molecules is an important process in astrophysics and fusion plasmas because it plays a crucial role for the energy loss, the charge state balance, and for the characterization of these plasmas as well as for many astronomical objects. Charge-transfer collisions involving carbon ions, in particular, are of practical importance because carbon ion is one of the major impurities in magnetic fusion plasma devices, and it is also one of the most abundant elements in astrophysical objects. A number of experiments on electron capture by partially stripped carbon ions have been carried out by several research teams in the last two decades [1–12]. However, charge-transfer reaction of C^{q+} and other solar wind ions such as O^{q+}, Si^{q+}, Ne^{q+}, and Fe^{q+} with molecules such as CO, CO_2, and H_2O from the comet atmosphere, has only recently been recognized as the primary mechanism for the observed soft x-ray and extreme ultraviolet emissions [13–21]. Qualitative modeling of cometary x-ray generated by charge-transfer process has been carried out by Cravens [22], Haberli *et al.* [23], and Kharchenko and Dalgarno [24]. A reasonable agreement was found between the measured emissions and the modeling. However, because very limited experimental data of relevance to cometary x-ray and EUV emission are available, the modeling was based on data extrapolated from the measured charge-transfer cross sections of O, C, and Ne ions with H and H_2. Only recently, measurements on charge transfer between solar wind ions such as C, N, O, Ne, and molecules such as CO [25,26], CO_2, and H_2O [27,28] have been performed experimentally. In this paper, we report measurements of total absolute single-electron-capture (SC) and double-electron-capture (DC) cross sections for C^{3+} and C^{4+} with CO. These charge-transfer processes are believed to be important contributors to the observed UV and EUV emissions of comets through cascading. Present measurements also suggest significant contribution from double-electron-capture processes to the observed emissions.

II. EXPERIMENTAL METHOD

The measurements were performed by a reflection time-of-flight mass spectrometer (RTOFMS) with a laser ablation ion source. Figure 1 is a simple sketch of the present experimental setup. A detailed description of the experimental facility can be found in Refs. [11,26]. Briefly, carbon ions C^{q+} ($q=3,4$) were produced by laser ablation of a high-purity (99.999%) solid Pyrolytic graphite target mounted on a rotatable manipulator inside the vacuum chamber. The energy of a 50 ns Nd:YAG laser pulse was about 180 mJ at 1.06 nm. The ions of the laser ablation plasmas were extracted into the incident drift tube through a small aperture of an extractor which marks the entrance to the RTOFMS. The extractor and the incident drift tube were both biased at $V_0 = -1500$ V relative to the ground. This extraction field creates different drift velocities for ions of different charge state in the incident field-free drift tube, because ions of charge q acquire additional kinetic energy, $\Delta E = -qeV_0$. Therefore, the ions of the same mass to charge ratio, (m/q), will bundle in space as they drift along the drift tube. They can be identified by their time-of-flight in the drift tube.

Ions produced by laser ablation, however, have a range of initial kinetic energies E_i. The spread of the kinetic energy of the same charge state ions limits the spatial resolution among ions of different m/q. Additional undertaking is necessary to focus the ions of same m/q at the plane of the detector. This is accomplished by reflecting the drifting ions in the incident drift tube by 168° into a reflection drift tube through a reflector assembly mounted at the end of the incident drift tube. The reflector assembly consists of a highly transparent front plate and a solid back plate. Between them, there are several evenly spaced potential-gradient ring electrodes to maintain a uniform electric field across the reflector assembly. With this, ions with higher initial kinetic energy penetrate further into the reflector assembly before they are reflected into the reflection drift tube. The extra path taken by the more energetic ions allows the slower ions to catch up in time. By choosing the appropriate potentials on the electrodes of the drift tube and the reflector assembly, ions of the same m/q but with different initial kinetic energies, can arrive at the incident plane of the CEM located at the far end of the reflection tube at about the same time [11].

The potentials of the front plate and the back plate of the reflector assembly were set at $V_1 = +15$ V and $V_2 = +900$ V, respectively. The range of initial kinetic energy E_i of the ions
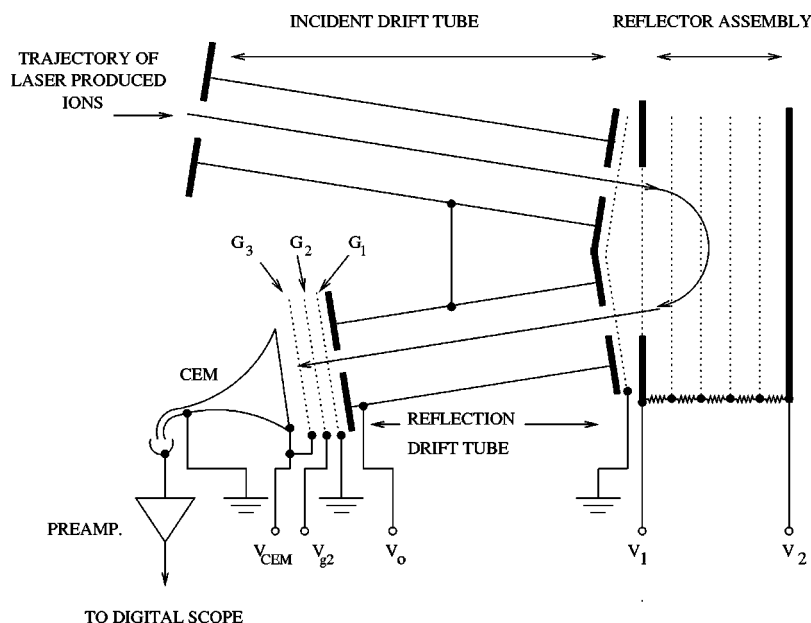
FIG. 1. A sketch of the reflector assembly and the reflection drift tube with a channel electron multiplier detector in the RTOFMS for electron-capture measurement.

reflected into the reflection drift tube was obtained by analyzing the trajectories of the reflected ions within the acceptance angle of the reflection drift tube. These ranges of E_i were found between 120 eV and 600 eV for C^{4+} ions, and between 80 eV and 400 eV for C^{3+} ions, respectively. The potentials applied to those electrodes were chosen for the optimum beam intensity and mass resolution. It is worthwhile to point out that any product ions, which are formed inside the incident drift tube by charge-transfer reaction between the carbon ions and molecules, cannot be reflected into the reflection drift tube. The kinetic energies of these product ions in the reflector region are greater than their parent ions by 1500 eV for SC and 3000 eV for DC due to the change of their charge states. Their trajectories after reflection are quite different from the parent ions. They are, therefore, beyond the angle acceptance of the reflection tube, and these product ions are blocked from entering the reflection drift tube. The parent carbon ions and only their product ions produced in the reflection drift tube by charge exchange reaction were detected by the CEM. Charge-transfer measurement, therefore, is carried out in the reflection drift tube region. The incident drift tube only serves as an integral part of the mass spectrometry for the laser produced ions.

A retardation field was applied between the end of the reflection drift tube and the CEM detector to separate the product ions from the parent ions (see Fig. 1). The ions lost their energies at the grounded grid 1 (G_1). Because of their charge state difference, the kinetic energies of the parent ions and their product ions, after passing through grid 1, were reduced to E_i, $E_i - eV_0$, and $E_i - 2eV_0$, for parent ions, C^{q+}, product ions formed by single electron capture, $C^{(q-1)+}$, and product ions formed by double electron capture, $C^{(q-2)+}$, respectively. By applying an appropriate potential barrier V_{g2} at grid 2 (G_2), selected carbon ions will be allowed to reach the CEM. For example, if $qeV_{g2} > E_i$ and $(q-1)eV_{g2} < E_i - eV_0$, C^{q+} will be blocked, $C^{(q-n)+}$ ($n \geqslant 1$) can pass through

grid 2 and be detected by the CEM. Similarly, $C^{(q-1)+}$ and $C^{(q-2)+}$ can be blocked with appropriate values of V_{g2}. The values of V_{g2} were set based on these E_i values and V_0. In the single-electron-capture measurement, the V_{g2} was set to 0 V, +595 V, +1600 V, respectively, for measuring the parent ions, all product ions $C^{(q-n)+}$ ($n \geqslant 1$), and the ions produced by multielectron capture $C^{(q-n)+}$ ($n \geqslant 2$). A higher voltage was used for double-electron-capture measurements, i.e., $V_{g2} = +1530$ V was used to measure product ions, $C^{(q-n)+}$ ($n \geqslant 2$), and $V_{g2} = 2200$ V for measuring the product ions formed by more than two-electron capture process, $C^{(q-n)+}$ ($n \geqslant 2$).

The target CO gas was admitted through a leak valve into the laser ablation vacuum chamber. The pressure of CO was measured by a calibrated ion gauge mounted at the reflection drift tube. The calibration method was discussed in a previous publication [29]. The CO pressure during the experiment was about 2.0×10^{-15} Torr. The residual gas pressure in the reaction chamber was less than 2.0×10^{-9} Torr.

The measurements were carried out in cycles to reduce the systematical uncertainty on the ion signal resulting from the laser energy fluctuation and the changes in the target surface conditions by laser ablation. In each cycle, V_{g2} was sequentially switched according to the calculated value set in the above discussion. About 3000 cycles were measured for SC or DC process, respectively. The signals were recorded by the Tektronix digital oscilloscope, binned according to the switching sequence, and stored in a computer for later analysis.

Figure 2 shows the typical TOF spectra in the measurement of the single electron capture. Two separate peak groups are located at about 1.8 μs and 3 μs, respectively, corresponding to C^{4+} and its product ions, C^{3+} and its product ions. Within each group, the largest peak, represented by a dashed line, corresponds to the parent ions and all their product ions and neutrals. While the much weaker peak, rep-
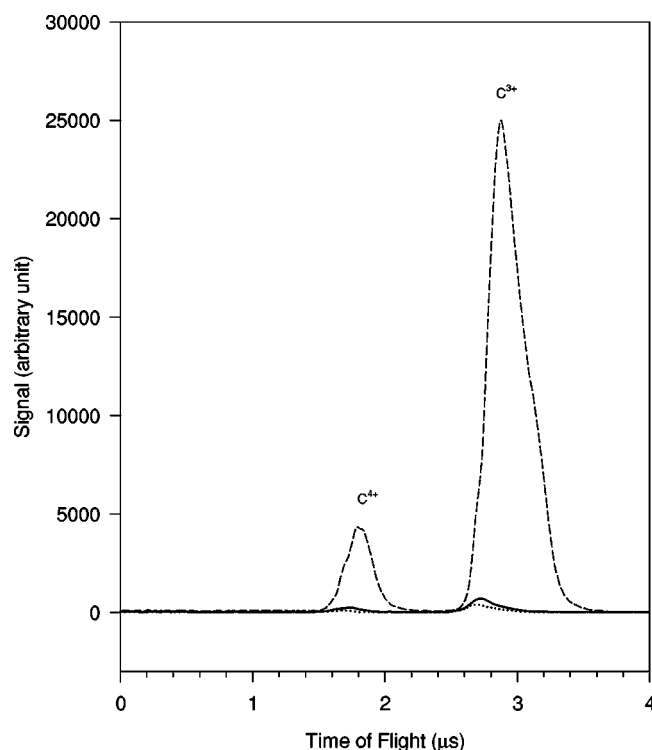
FIG. 2. Typical time-of-flight mass spectra in the measurement of the single and double electron capture of C^{3+} and C^{4+} with CO. Signal at 3 μs, from large to small: laser produced parent C^{3+} ions; all product ions including C^{2+}, C^+, and C; and product ions excluding C^{2+}. Signal at 1.8 μs, from large to small: laser produced parent C^{4+} ions; all product ions including C^{3+}, C^{2+}, C^+, and C; and product ions excluding C^{3+}.

resented by a solid line, corresponds to all the product ions and the neutrals, $C^{(q-n)+}$ ($n \geq 1$). The smallest peak, represented by a dotted line, corresponds to the product ions and the neutrals formed by multielectron capture processes, $C^{(q-n)+}$ ($n \geq 2$). These signal intensities were used to determine the charge-transfer cross sections.

III. RESULTS AND DISCUSSION

The electron capture cross section, σ, can be derived from the following expression:

$$I_p/I_0 = 1 - e^{-\sigma nL}, \tag{1}$$

$$\sigma \cong I_p/(I_0 nL), \tag{2}$$

where I_p is the signal intensity of the product carbon ions, I_0 is the intensity of the parent C^{q+} ions, L is the interaction length of the reflection drift tube, and n is the density of the target CO gas. In Eq. (2), the approximation is valid because $I_p/I_0 \ll 1$ in our measurement, which also ensures single collision condition. The mean ion energies are estimated to be 6780±780 eV and 5076±576 eV for C^{4+} and C^{3+}, respectively. The measured charge-transfer cross sections are tabulated in Table I. Results of previous measurements with H_2 and CO_2 [2,3,5,7,12] are also listed in the table for comparison.

One of the major experimental uncertainties comes from the gain efficiency of the detector, which depends on the ion charge state and its incident kinetic energy [2]. Because CEM was operated in the analog mode, the gain efficiencies for C^{q+} ($q=4,3,2,1$) needs to be calibrated. The calibration procedure has been discussed in our previous publications [11,26]. It turns out that the difference in the efficiency with carbon ions and oxygen ions, which we measured previously is within 10% [26]. Other sources contributed to the experimental uncertainty include (1) 8% from the gas pressure for the absolute ion gauge calibration; (2) 2% introduced from the nonlinearity of the channel electron multiplier and the preamplifier; and (3) the statistical uncertainties of the measured cross sections: it is about 6% for single electron capture and 8% for double electron capture. The quadrature sum of the uncertainties give a total absolute uncertainty of 14% for single electron capture and 15% for double-electron-capture cross section.

In the low-energy collision regime, it is well known that the electron-capture cross section strongly depends on the internal electronic state of the ions. The presence of metastable state ions in the parent ion beam make the interpretation of result very difficult. C^{3+} is Li-like. Its metastable state ($1s2s2p\ ^4P_J$) lifetime has been measured to be 2.3 ns and 129 ns for $J=1/2$ and 5/2, respectively [30]. While no measurement is available for $j=2/3$, the lifetime can be extrapolated from the corresponding $j=2/3$ lifetime of N^{4+} and O^{5+} [30]. Nevertheless, their lifetimes are too short to reach the reflection drift tube where the charge-transfer measurement is carried out.

The radiative lifetime of the $1s2s\ ^1S$ and $1s2s\ ^3S$ metastable states of C^{4+} ion has been calculated to be about 3 μs and 112 s, respectively [31]. Recent measurement, however, gives only 20.59 ms for $1s2s\ ^3S$ [32]. Nonetheless, both their lifetimes are much longer than the flight time of the ion inside the RTOFMS. The 1.8 μs transit time does not allow C^{4+} ions to relax to their ground state prior to the measurements if they are present in the beam. The presence of long-lived metastable fraction in ion beam has been found in several ion beam experiments using an ion-impact ion-source [7], an ECR ion source [5], or a PIG ion source [2]. The metastable fraction can account for as much as 5–32% of the ion beam. These metastable ions are created by electron impact ionization and excitation of the carrier gas.

In the present experiment, a laser induced plasma ion source is used. This is a pulsed ion source where the ions freely expand into the vacuum before they are extracted for the measurement. Ions created by laser ablation of a solid target are initially hot due to rapid collision with high-density laser heated plasma electrons [33–36]. During the early expansion phase of the plasma, collisional equilibrium is established between the plasma electrons and the ionic and atomic species in the plasma. The internal temperature of these heavy species is closely coupled to the temperature of the plasma electrons. As the temperature of the plasma electron drops when its energy is converted to its directed energy of expansion, the internal temperature of the atomic and ionic species cools. Since the electron density n_e is $\propto t^{-3}$ while the electron temperature T_e is $\propto t^{-1}$ [34], the internal temperature of the atomic and ionic species freezes out when

TABLE I. Measured charge transfer cross section σ for C^{q+} ($q=3,4$) with CO, CO_2, and H_2.

Reaction	Energy (eV/amu)	$\sigma(SC)^a$ (10^{-15} cm^2)	$\sigma(DC)^b$ (10^{-15} cm^2)	Reference	Method
$C^{3+}+CO$	423 ± 48	0.96 ± 0.12	0.99 ± 0.13	This work	c
$C^{3+}+H_2$	161	0.56 ± 0.29		[2]	d
	192	0.77 ± 0.06	0.45 ± 0.04	[7]	e
	358	0.71 ± 0.06	0.36 ± 0.03	[7]	
	525	0.64 ± 0.05	0.36 ± 0.03	[7]	
$C^{3+}+CO_2$	692	1.0 ± 0.1	0.97 ± 0.10	[7]	
	1750	1.1 ± 0.1	1.2 ± 0.1	[27]	f
$C^{4+}+CO$	565 ± 65	3.16 ± 0.42	1.05 ± 0.21	This work	c
$C^{4+}+H_2$	387	3.91 ± 0.87		[2]	d
	358	2.60 ± 0.18	0.31 ± 0.03	[7]	e
	832	2.44 ± 0.12		[3]	f
	1692	2.30 ± 0.16	0.24 ± 0.02	[7]	
	520	3.87 ± 0.40^g		[5]	f
	583	3.26 ± 0.33^g		[5]	
	600	3.55 ± 0.15^g		[12]	f

[a]SC, single electron capture.
[b]DC, double electron capture.
[c]RTOFMS and laser ion source.
[d]ORNL-PIG ion source.
[e]Ion-Impact ion source.
[f]ECR ion source.
[g]Capture into $3l$ subshell only.

n_e drops below the threshold density to maintain collisional equilibrium. The freeze out temperature of a laser induced plasma seeded with neutral chromium was first investigated by Drewell [36]. The investigation was carried out by the simultaneous laser selective excitation of the $a\,^5S_2$ metastable and the $a\,^7S_3$ ground state of Cr. His finding reveals the freeze out population ratio between $a\,^5S_2$ metastable state and the $a\,^7S_3$ ground state to be about 10^{-3}. This is consistent with the result obtained by Fang and Kwong [37,38] and Wang and Kwong [11] on the metastable fraction of laser produced O^{2+} and C^{2+} ions. Since the power and energy of the ablation laser used by Drewell [36] is similar to our measurement, and the $a\,^5S_2$ metastable state of Cr is only 0.94 eV above its $a\,^7S_3$ ground state, it is reasonable to assume that the $1s2s\,^1S$ and $1s2s\,^3S$ (both are ~300 eV above the $1s^2\,^1S$ ground state) metastable fraction of the laser produced C^{4+} ions is much less than 10^{-3}. We conclude that there is no significant metastable state contribution to the measured cross section in the present measurements.

Since neither theoretical nor experimental cross sections are available for CO, the electron capture cross sections are first compared to those estimated by the classical over-barrier model (CBM); and then the SC cross sections are compared with those with H_2, because the modeling of x-ray emission from comet atmosphere was based on electron-capture cross sections of H_2 [23].

The static classical over-barrier model (CBM) was first proposed by Ryufuku et al. [39] for estimating electron-capture cross section. It was later extended to estimate the cross section for consecutive multiple electron transfer process by Barany [40] and Niehaus [41]. This model has been proven to be fairly successful in predicting the total charge-transfer cross section in collision of slow highly charged ion with hydrogen. In CBM [39], capture is assumed to occur at an internuclear distance R_c when charge transfer becomes classically allowed and the capture electron predominantly into one specific shell, n, which is the largest integer satisfying the inequality,

$$n \leq q\{(2q^{1/2}+1)/[2I_t(q+2q^{1/2})]\}^{1/2},$$

where q is the charge state of the projectile and I_t is the ionization potential in atomic units of the target gas. The crossing radius for the over-barrier transition for hydrogenic system can be expressed as

$$R_c = 2(q-1)/(q^2/n^2 - 2I_t).$$

The magnitude of the cross section is determined by πR_c^2. In the extended CBM, the two-electron transfer may be expressed as $\pi(R_2^2 - R_3^2)$ [40] with

$$R_m = \{2([q-m+1]m)^{1/2} + m\}/I_m,$$

where I_m is the mth ionization potential of the target gas.

In the single electron capture reaction of C^{q+} with CO, this model predicts that electron is captured into $n=2$ and $n=3$ shells for $q=3$ and 4, respectively. The SC cross sections are estimated to be 0.95×10^{-15} cm^2 and 5.66×10^{-15} cm^2 for C^{3+} and C^{4+}, respectively. Using the double and triple ionization potentials of CO [42], the DC cross sections are estimated to be about 1.17×10^{-15} cm^2 and

1.48×10^{-15} cm^2 for C^{3+} and C^{4+}, respectively. The overall agreement is within a factor of two of our measurement. It is however worthwhile to point out that good agreement should not be expected because (1) a quasi continuum of unoccupied energy states of the projectile ion is not satisfied for low n states, and (2) the complex structure of the target CO molecule.

In Table I, two sets of cross section with H$_2$ are listed: The data measured by Phaneuf *et al.* [2] used in the x-ray emission modeling of cometary atmosphere and the data measured by Itoh *et al.* [7]. The cross sections measured by Itoh *et al.* shows little dependence on the collision energies between 100 eV/amu and 1690 eV/amu [7]. For C^{3+}, these two measurements agree with each other to within the measurement uncertainties. However, the C^{4+} cross sections measured by Itoh *et al.* [7] and Phaneuf *et al.* [2] differ by more than one standard deviation of the measurement error. Furthermore, the cross sections measured by Itoh *et al.* [7] are smaller than the dominant partial cross section ($3l$ subshell) measured by Hoekstra *et al.* [5] and Lubinski *et al.* [12] at similar energies.

Comparing the present SC cross sections of C^{q+} ($q = 3,4$) with CO and that with H$_2$, it appears to be no significant difference for both C^{3+} and C^{4+} within the experimental uncertainties. The DC cross sections for C^{3+} and C^{4+} with H$_2$ measured by Itoh *et al.* [7] are about 51% and 12% of that for SC, respectively. However, in the reaction of C^{q+} ($q = 3,4$) with CO, the DC cross sections are as much as 102% and 30% of that of SC for C^{3+} and C^{4+}, respectively. Furthermore, the DC reactions for C^{q+} with CO are faster by a factor of three than their respective reactions with H$_2$. Finally, from Table I, the present measured SC and DC cross sections of C^{3+} with CO are similar to that of CO$_2$ measured at a higher energy [7,27]. Since CO$_2$ is also found in comet atmosphere, and both DC reactions are as fast as that of SC, DC process should not be ignored in the modeling comet emissions.

[1] D. H. Crandall, R. A. Phaneuf, and F. W. Meyer, Phys. Rev. A **19**, 504 (1979).

[2] R. A. Phaneuf, I. Alvarez, F. W. Meyer, and D. H. Crandall, Phys. Rev. A **26**, 1892 (1982).

[3] D. Dijkkamp, D. Ciric, E. Vlieg, A. de Boer, and F. J. de Heer, J. Phys. B **18**, 4763 (1985).

[4] H. Cederquist, L. H. Andersen, A. Barany, P. Hvelplund, H. Knudsen, E. H. Nielsen, J. O.K. Pedersen, and J. Sorensen, J. Phys. B **18**, 3951 (1985).

[5] R. Hoekstra, J. P.M. Beijers, A. R. Schlatmann, and R. Morgenstern, Phys. Rev. A **41**, 4800 (1990).

[6] T. K. McLaughlin, R. W. McCullough, and H. B. Gilbody, J. Phys. B **25**, 1257 (1992).

[7] A. Itoh, N. Imanishi, F. Fukuzawa, N. Hamamoto, S. Hanawa, T. Tanaka, T. Ohdaira, M. Satto, Y. Haruyama, and T. Shirai, J. Phys. Soc. Jpn. **64**, 3255 (1995).

[8] C. C. Havener, A. Muller, P. A. Zeijlmans Van Emmichoven, and R. A. Phaneuf, Phys. Rev. A **51**, 2982 (1995).

[9] F. W. Bliek, R. Hoekstra, M. E. Bannister, and C. C. Havener, Phys. Rev. A **56**, 426 (1997).

[10] M. O. Larsson, A. Wannstrom, M. Wang, A. Arnesen, F. Heijkenskjold, A. Langereis, B. Nystrom, R. W. McCullough, and H. Cederquist, Phys. Rev. A **55**, 1911 (1997).

[11] J. Wang and V. H. S. Kwong, Rev. Sci. Instrum. **68**, 3712 (1997).

[12] G. Lubinski, Z. Juhasz, R. Morgenstern, and R. Hoekstra, J. Phys. B **33**, 5275 (2000).

[13] C. M. Lisse, K. Dennerl, J. Englhauser, M. Harden, F. E. Marshall, M. J. Mumma, R. Petre, J. P. Pye, M. J. Ricketts, J. Schmitt, J. Trumper, and R. G. West, Science **274**, 205 (1996).

[14] C. M. Lisse, K. Dennerl, J. Englhauser, J. Trumper, F. E. Marshall, R. Petre, A. Valinia, B. J. Kellett, and R. Bingham, Earth, Moon, Planets **77**, 283 (1999).

[15] C. M. Lisse, D. Christian, K. Dennerl, J. Englhauser, J. Trumper, M. Desch, F. E. Marshall, R. Petre, and S. Snowden, Icarus **141**, 316 (1999).

[16] K. Dennerl, J. Englehauser, and J. Trumper, Science **277**, 1625 (1997).

[17] V. A. Krasnopolsky, M. J. Mumma, M. Abbott, B. C. Flynn, K. J. Meech, D. K. Yeomans, P. D. Feldman, and C. B. Cosmovici, Science **277**, 1488 (1997).

[18] M. J. Mumma, V. A. Krasnopolsky, and M. J. Abbott, Astrophys. J. Lett. **491**, L125 (1997).

[19] A. Owens, A. N. Parmar, T. Oosterbroek, A. Orr, L. A. Antonelli, F. Fiore, R. Schulz, G. P. Tozzi, M. C. Maccarone, and L. Piro, Astrophys. J. Lett. **493**, L47 (1998).

[20] C. M. Lisse, D. J. Christian, K. Dennerl, K. J. Meech, R. Petre, H. A. Weaver, and S. J. Wolk, Science **292**, 1343 (2001).

[21] V. A. Krasnopolsky and M. J. Mumma, Astrophys. J. **549**, 629 (2001).

[22] T. E. Cravens, Geophys. Res. Lett. **24**, 105 (1997).

[23] R. M. Haberli, T. I. Gombosi, D. L. De Zeeuw, M. R. Combi, and K. G. Powell, Science **276**, 939 (1997).

[24] V. Kharchenko and A. Dalgarno, Astrophys. J. Lett. **554**, L99 (2001).

[25] H. Gao, Z. Fang, and V. H. S. Kwong, Phys. Rev. A **63**, 032704 (2001).

[26] H. Gao and V. H. S. Kwong, Astrophys. J. **567**, 1272 (2002).

[27] J. B. Greenwood, I. D. Williams, S. J. Smith, and A. Chutjian, Astrophys. J. Lett. **533**, L175 (2000); Phys. Rev. A **63**, 062707 (2001).

[28] A. A. Hasan, F. Eissa, R. Ali, D. R. Schultz, and P. C. Stancil, Astrophys. J. Lett. **560**, L201 (2001).

[29] V. H. S. Kwong *et al.*, Rev. Sci. Instrum. **61**, 1931 (1990).

[30] D. Charalambidis, R. Brenn, and K. J. Koulen, Phys. Rev. A **40**, 2359 (1989).

[31] G. W. F. Drake, G. A. Victor, and A. Dalgarno, Phys. Rev. **180**, 25 (1969).

[32] H. T. Schmidt, P. Forck, M. Grieser, D. Habs, J. Kenntner, G. Miersch, R. Repnow, U. Schramm, T. Schussler, D. Schwalm, and A. Wolf, Phys. Rev. Lett. **72**, 1616 (1994).

[33] J. M. Dawson, Phys. Fluids **7**, 981 (1964).

[34] P. T. Rumsby and J. W. Paul, Plasma Phys. **16**, 247 (1974).

[35] R. M. Measures, N. Drewell, and H. S. Kwong, Phys. Rev. A **16**, 1093 (1977).

[36] N. Drewell, Ph.D. thesis, University of Toronto, Toronto, Ontario, Canada (1979), p. 48–53.

[37] Z. Fang and V. H. S. Kwong, Rev. Sci. Instrum. **65**, 2143 (1994).

[38] Z. Fang and V. H. S. Kwong, Phys. Rev. A **51**, 1321 (1995).

[39] H. Ryufuku, K. Sasaki, and T. Watanabe, Phys. Rev. A **21**, 745 (1980).

[40] A. Barany *et al.*, Nucl. Instrum. Methods Phys. Res. B **9**, 397 (1985).

[41] A. Niehaus, J. Phys. B **19**, 2925 (1986).

[42] P. Lablanquie *et al.*, Phys. Rev. A **40**, 5673 (1989).